Vaclav KUS
Tereza JOSEFOVA

COMPARISON OF TWO ANALYTICAL CALCULATIONS OF HARMONIC ANALYSIS OF THE CURRENT DRAWN BY THE VOLTAGE-SOURCE ACTIVE RECTIFIER FROM THE ELECTRICAL GRID

SUMMARY *Voltage-source active rectifier eliminates characteristics harmonics, which are drawn by diode (thyristor) rectifiers from the electrical grid. The paper shows analytical analysis of the current drawn from the grid by voltage-source active rectifier. The first part presents the principle of the voltage-source active rectifier. The next part describes both analyses of the current and the last part shows comparison of both analyses with simulations.*

Keywords: *voltage-source active rectifier, harmonic analysis, frequency modulation, Fourier analysis*

1. INTRODUCTION

Large increase in frequency converters with classic diode rectifiers causes problems with high values of current harmonics drawn from the grid; these harmonics are called characteristic harmonics [1-3]. A way to eliminate these harmonics (besides the classical filtration equipment [4, 5]) is to use active rectifier. Voltage-source active rectifier minimizes the characteristic harmonics, but new harmonics appear in the spectrum of current drawn from the grid by this rectifier. These new harmonics are dependent on the switching frequency. The paper shows that the primarily frequencies, which are identical to switching frequency or derived from the switching frequency occur in the spectrum of the current. At the same time, the first measurements occur in the practice that complements our findings [6].

Prof. Ing. Vaclav KUS CSc., Ing. Tereza JOSEFOVA
e-mail: kus@kev.zcu.cz; terkajos@kev.zcu.cz

University of West Bohemia, Department of Electromechanics and Power Electronics

2. PRINCIPLE OF THE VOLTAGE-SOURCE ACTIVE RECTIFIER

Voltage-source active rectifier has a similar structure as inverter. It is composed of six switches; each switch is formed by IGBT and antiparallel diode. Voltage-source active rectifier has DC side connected with capacitor (Fig. 1). Constant voltage is maintained on this capacitor [6].

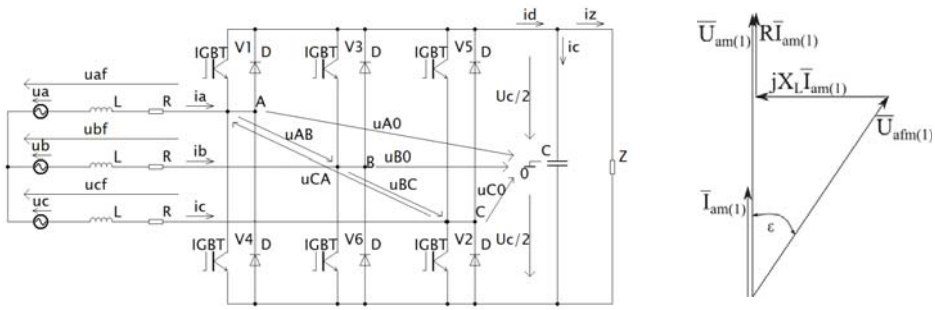

Fig. 1. Three-phase voltage-source active rectifier and its Phasor diagram

2.1. Voltage Type Control on the DC Side

The basis for the control voltage type is phasor diagram, where the first harmonic of current drawn from the grid is in phase with the first harmonic of supply voltage (Fig. 1). This phasor diagram is derived from the Kirchhoff's voltage law that is written for phase *a*:

$$\overline{U_{am(1)}} - jX_{La}\overline{I_{am(1)}} - R\overline{I_{am(1)}} - \overline{U_{afm(1)}} = 0 \tag{1}$$

The angle of the control ε is the phase shift of the first harmonic of supply voltage $U_{am(1)}$ and the first harmonic of phase voltage of the grid $U_{afm(1)}$ (Fig. 1 and 2). The angle of the control increases with the increasing load on the DC side of the active rectifier and the requirement to increase the current drawn from the grid is specified. More about active rectifier and its control can be found in the publications [7-9].

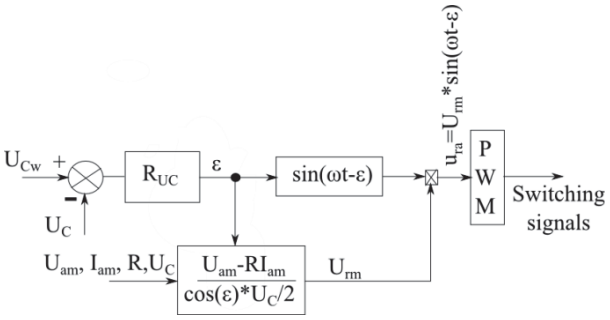

Fig. 2. The regulatory scheme of the voltage-source active rectifier

The symbols in the Figure 2: U_{Cw} is desired value of capacitor voltage, U_C is real value of capacitor voltage, R_{UC} is regulator of capacitor voltage, ε is angle of the control, U_{am} and I_{am} are first harmonics of supply voltage and supply current, R is resistance, u_{ra} is control voltage of pulse width modulation (PWM), U_{rm} is amplitude of control voltage.

Proper functioning of the active rectifier is depicted in the Figure 3, which also shows the current drawn from the grid in phase with the supply voltage. The current waveform is composed of individual sections, which approximate an increasing or a decreasing exponential function. Simulation of voltage-source active rectifier with the voltage type control was created in C language.

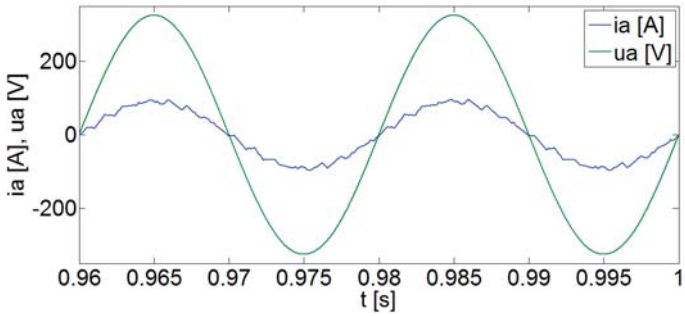

Fig. 3. Current drawn from the grid, in phase with the supply voltage

3. INTRODUCTION OF THE THEORY OF THE FREQUENCY MODULATION TO THE EXPONENTIAL FOURIER SERIES

In the theory of frequency modulation the carrier harmonic signal is:

$$u_s(t) = U_s \cdot \sin(\omega t + \varphi), \tag{2}$$

where U_s is the amplitude of the carrier signal and ω is the frequency of the carrier signal and φ is the phase. Frequency modulation is characterized by changing the intensity of the modulation signal at a frequency ω_m. The angular frequency $\omega(t)$, which can be expressed as a harmonic function of time, is:

$$\omega(t) = \omega_s + \Delta\omega_s \cdot \cos(\omega_m t), \tag{3}$$

The introduction of the modulation index m_F of the frequency modulation:

$$m_F = \frac{\Delta\omega_s}{\omega_m} = \frac{2\pi\Delta f_s}{2\pi f_m} \tag{4}$$

In accordance with the basic definition of $\omega = \frac{d\varphi}{dt}$ it is possible to write:

$$\varphi = \int \omega dt = \int \big(\omega_s + \omega_m m_F \cdot \cos(\omega_m t)\big)dt = \omega_s t + m_F \sin(\omega_m t) \tag{5}$$

By substituting $\varphi(\omega,t)$ and the modulation index m_F into the equation of the carrier signal (2) we get:

$$u_s = U_s \cdot \{\sin(\omega_s t) \cdot \cos[m_F \cdot \sin(\omega_m t)] + \cos(\omega_s t) \cdot \sin[m_F \cdot \sin(\omega_m t)]\} \tag{6}$$

The function from (6) can be developed in Fourier series:

$$\begin{aligned} \cos\big(z \cdot \sin(v)\big) &= J_0(z) + 2\sum_{p=1}^{\infty} J_{2p}(z) \cdot \cos(2pv) \\ \sin\big(z \cdot \sin(v)\big) &= 2\sum_{q=1}^{\infty} J_{2q-1}(z) \cdot \sin\big((2q-1)v\big) \end{aligned} \tag{7}$$

Equation (6) is rewritten in accordance with (7) ($z = m_F$ and $v = \omega_m t$):

$$\begin{aligned} u_S = U_S \cdot [&J_0(m_F) \cdot \sin(\omega_s t) + (2 \cdot J_1(m_F) \cdot \sin(\omega_m t) \cdot \cos(\omega_s t) + \\ &+2 \cdot J_2(m_F) \cdot \sin(\omega_s t) \cdot \cos(2\omega_m t) + 2 \cdot J_3(m_F) \cdot \sin(3\omega_m t) \cdot \cos(\omega_s t) + \\ &+2 \cdot J_4(m_F) \cdot \sin(\omega_s t) \cdot \cos(4\omega_m t) + \cdots] \end{aligned} \tag{8}$$

where $J_h(m_F)$ are Bessel function which are:

$$\begin{aligned} J_h(m_F) &= \Big(\frac{m_F}{2}\Big)^h \sum_{r=0}^{\infty} \frac{(-1)^r}{r!\,(r+h)!}\Big(\frac{m_f}{2}\Big)^{2r} \\ J_{-h}(m_F) &= (-1)^n J_h(m_F) \end{aligned} \tag{9}$$

Equation (8) can be modified as:

$$u_s(t) = U_s \cdot \sum_{h=-\infty}^{\infty} J_h(m_F) \cdot \sin\big((\omega_s + h\omega_m)t\big) \tag{10}$$

In the case of purely sinusoidal modulation the amplitude spectrum of components is symmetrical and unlimited, it is the frequency: ω_s - $h\omega_m$, ..., ω_s - $2\omega_m$, ω_s - ω_m, ω_s, ω_s + ω_m, ... For $m_F > 5$ the bandwidth is:

$$B \geq 2(f_s + 2f_m) \tag{11}$$

Exponential Fourier series is:

$$u_v(t) = \sum_{h=-\infty}^{\infty} c_h \cdot e^{jh\omega t}, \tag{12}$$

where coefficient of exponential Fourier series c_h is [10, 11]:

$$c_h = \frac{1}{T}\int_0^T u_v(t) \cdot e^{-jh\omega t}\, dt \tag{13}$$

Now the results from frequency modulation are used; PWM signal is replaced by cosine modulation with frequency ω_m. Relation (5) is substituted into equation (12) [12]:

$$\begin{aligned} u_v(t) &= \sum_{h=-\infty}^{\infty} c_h \cdot e^{jh\omega t} = \sum_{h=-\infty}^{\infty} c_h \cdot e^{jh\varphi_h} \\ &= \sum_{h=-\infty}^{\infty} c_h \cdot e^{jh2\pi f_s t} \cdot \begin{Bmatrix} \cos \cdot [hm_F \cdot \sin(2\pi f_m t)] \\ +\mathrm{j}\sin \cdot [hm_F \cdot \sin(2\pi f_m t)] \end{Bmatrix} \end{aligned} \tag{14}$$

Final equation of exponential Fourier series is:

$$\begin{aligned} u_v(t) = \sum_{h=-\infty}^{\infty} c_h \{ & J_0(hm_F) e^{j2\pi h f_s t} + \sum_{k=1}^{\infty} J_k(hm_F) \\ & \cdot \left[e^{j2\pi(kf_s + kf_m)t} + (-1)^k e^{j2\pi(kf_s - kf_m)t} \right] \} \end{aligned} \tag{15}$$

In accordance with the result of (14), the spectrum of the PWM signal is composed of groups of harmonics around integer multiples of the switching frequency f_{sw}. Around each k-multiple there are sidebands of the harmonics. Spacing is equal to k-multiples of the modulation frequency f_m. In accordance with the implementation of (11) it can be written:

$$\begin{aligned} \boldsymbol{B_h} &= \boldsymbol{(2km_F + 1)f_m} \\ \Delta \boldsymbol{f_h} &= \boldsymbol{kf_s \pm f_m} \end{aligned} \tag{16}$$

4. CALCULATIONS OF THE AMPLITUDE OF CURRENT HARMONICS USING PIECEWISE LINEARIZED CURRENT WAVEFORM

The Figure 4 shows correct functioning of the three-phase voltage-source active rectifier. Phase voltage of the grid u_{af} is obviously dependent on the phase voltages of the active rectifier u_{A0} and u_{B0} and equals values $\pm U_C/3$, $\pm 2U_C/3$ and 0 according to the following formula [13]:

$$u_{af} = \frac{1}{3}\left(2u_{A0} - u_{B0} - u_{C0}\right) \tag{17}$$

Current increases and decreases several times during one polarity of the phase voltage of the active rectifier u_{A0}.

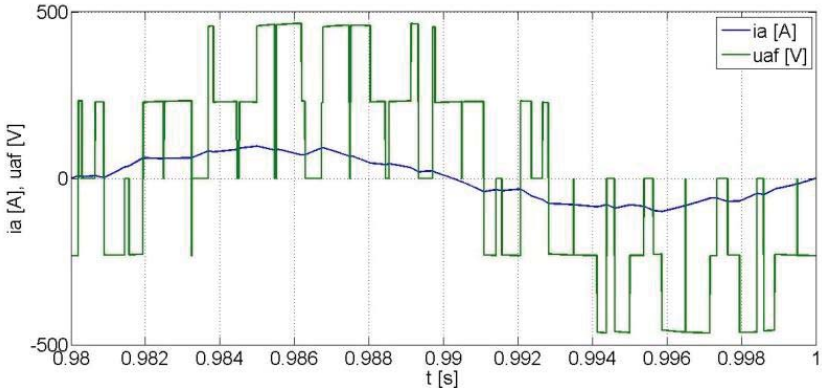

Fig. 4. Current drawn from the grid i_a and phase voltage of the grid u_{af} during proper functioning of the rectifier

Voltage u_{af} divides the current waveform drawn from the grid into sections, in which the current approximates an increasing or a decreasing exponential function (Fig. 5a). The sections were linearized, i.e. they were replaced by increasing or decreasing straight lines (Fig. 5b).

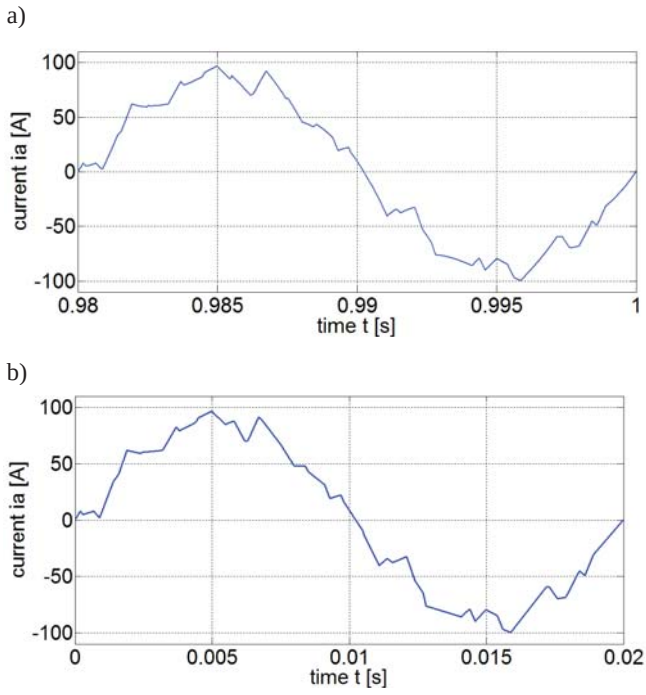

Fig. 5. Current drawn from the grid i_a during proper functioning of the rectifier (a) and piecewise linearized current waveform (b)

Piecewise linearized current waveform was accepted for analytical calculation of the Fourier coefficients, which were then used to calculate harmonic analysis. Fourier coefficients were calculated for each individual section and thereafter they were summed for all parts (straight lines) of the waveform (Fig. 6).

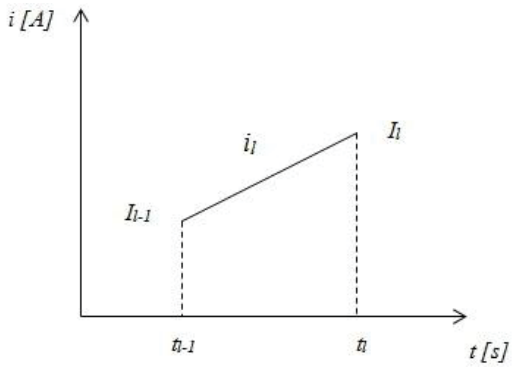

Fig. 6. Description of the l-th straight line from the simplified current waveform

Equation of the l-th straight line:

$$i_l = c_l t + d_l \tag{18}$$

Equation for the member c_l from the l-th straight line:

$$c_l = \frac{I_l - I_{l-1}}{t_l - t_{l-1}} \tag{19}$$

Equation for the member d_l from the l-th straight line:

$$d_l = I_{l-1} - c_l \cdot t_{l-1} \tag{20}$$

Calculation of Fourier coefficient a_{hl} for n-th straight line of simplified current waveform:

$$a_{hl} = \frac{2}{T}\int_{t_{l-1}}^{t_l}\left(c_l t + d_l\right)\cos\left(h\omega t\right)dt = \frac{2}{T}\frac{c_l}{h\omega}\left[t\sin\left(h\omega t\right) + \frac{1}{h\omega}\cos\left(h\omega t\right) + \frac{d_l}{c_l}\sin\left(h\omega t\right)\right]_{t_{l-1}}^{t_l} \tag{21}$$

Calculation of Fourier coefficient b_{hl} for l-th straight line of simplified current waveform:

$$b_{hl} = \frac{2}{T}\int_{t_{l-1}}^{t_l}\left(c_l t + d_l\right)\sin\left(h\omega t\right)dt = \frac{2}{T}\frac{-c_l}{h\omega}\left[t\cos\left(h\omega t\right) - \frac{1}{h\omega}\sin\left(h\omega t\right) + \frac{d_l}{c_l}\cos\left(h\omega t\right)\right]_{t_{l-1}}^{t_l} \tag{22}$$

The resulting members a_h and b_h for all simplified current waveform:

$$a_h = \sum_{l=1}^{\infty} a_{hl} \tag{23}$$

$$b_h = \sum_{l=1}^{\infty} b_{hl} \tag{24}$$

The resulting Fourier series:

$$f(t) = \frac{a_0}{2} + \sum_{h=1}^{\infty}\left[\left(\sum_{l=1}^{\infty} a_{hl}\right)\cos(h\omega t) + \left(\sum_{l=1}^{\infty} b_{hl}\right)\sin(h\omega t)\right] \tag{25}$$

The amplitude of the h-th harmonic of the current:

$$I_h = \sqrt{a_h^2 + b_h^2} \tag{26}$$

4.1. The Comparison of the analytical calculations and the simulations

The next graphs (Fig. 7) show the comparison of harmonic analysis of the correct current waveform from the Figures 4 and 5a and of harmonic analysis of the piecewise linearized current waveform from the Figure 5b.

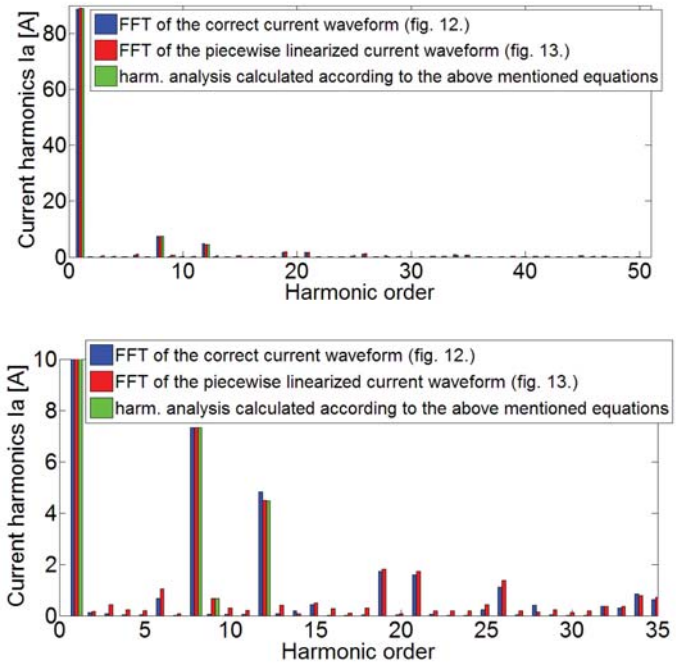

Fig. 7. The comparison of individual harmonic analysis

If we analyze the Figures 7, we can see especially the harmonics that are close to the switching frequency (f_{sw} = 500Hz) and its multiple in the spectrum of the current (16). It is also evident that the harmonic analysis error rate is almost negligible (less than 1%) even in case of linearization of the current waveform. This is due to higher amount of sections in which the current waveform is divided. The error rate will be smaller, when the switching frequency will be higher.

5. CALCULATION OF AMPLITUDE OF CURRENT HARMONICS USING THE VOLTAGE OF THE ACTIVE RECTIFIER

To calculate the current harmonics drawn from the grid by three-phase voltage--source active rectifier the phase voltage of the grid u_{af}, which equals 0, $\pm U_C/2$, $\pm U_C/3$ is divided into individual phase voltages of the active rectifier u_{A0} (Fig. 8), u_{B0} and u_{C0}, which equal $\pm U_C/2$ according to the mentioned equation (17). To calculate the size of current harmonics drawn from the grid, only the current i_{A0} that is formed by voltage u_{A0} will be taken into account. Further the individual harmonics of the currents i_{A0}, i_{B0} and i_{C0} are summed, thus calculating the harmonics of the current drawn from the grid i_a [12].

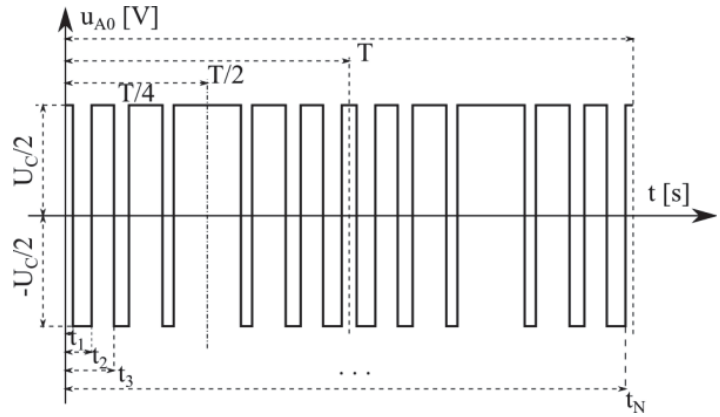

Fig. 8. Description of the whole period of the PWM signal of the voltage

The voltage waveform can be described as follows:

$$u_{A0}(t) = \frac{U_c}{2} \qquad t \in (0, t_1), (t_2, t_3), ..., (t_N, T)$$

$$u_{A0}(t) = -\frac{U_c}{2} \qquad t \in (t_1, t_2), (t_3, t_4), ..., (t_{N-1}, t_N)$$

Calculation of the coefficient a_h of Fourier series:

$$a_h = \frac{2}{T}\int_0^T u_{A0}(t)\cdot\cos(h\omega t)\,dt$$
$$a_{uA0h} = \frac{Uc}{Th\omega}\left[\sum_{k=1}^{N}(-1)^{k+1}\,2\sin(h\omega t_k)\right] \tag{27}$$

Calculation of the coefficient b_h of Fourier series:

$$b_h = \frac{2}{T}\int_0^T u_{A0}(t)\cdot\sin(h\omega t)\,dt$$
$$b_{uA0h} = \frac{U_c}{Th\omega}\left[\sum_{k=1}^{N}(-1)^{k}\,2\cos(h\omega t_k)\right] \tag{28}$$

Calculation of harmonics of the voltage u_{A0}:

$$U_{A0(h)} = \sqrt{a_{uA0h}^2 + b_{uA0h}^2}\,[V] \tag{29}$$

The results of harmonic analysis of voltage waveform, which is created using pulse width modulation, are used to calculate the harmonics current. In the next section, we assume some simplifying conditions:

- supply voltage is sinusoidal and contains only the first harmonic;
- the voltage on DC side of the active rectifier is ideally smoothed with the value U_C;
- symmetry elements and their switching are maintained;
- transistors switch immediately after supplying switching pulse;
- rectifier control is based on the principle of PWM modulation only for the first harmonic – moments of switching transistors correspond to moments of coincidence of modulation voltage and carrier signal, dead times are not considered during the control of the active rectifier.

Based on these requirements and the description of the principle of the voltage--source active rectifier the equivalent circuit can be drawn for the AC side of the active rectifier (Fig. 9).

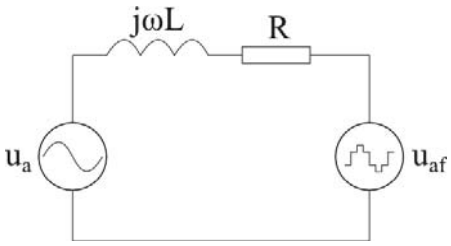

Fig. 9. Equivalent circuit of the active rectifier

The voltage on the input side u_{af} is spread over voltages u_{A0}, u_{B0} and u_{C0} and is directed against main voltage u_a. According to the equivalent circuit in Fig. 9, we can write an equation for the harmonics $I_{A0(h)}$:

$$I_{A0(h)} = \frac{U_{A0(h)}}{h\omega_1 L} = \frac{\sqrt{a_{uA0h}^2 + b_{uA0h}^2}}{h\omega_1 L} \tag{30}$$

First harmonic of the current $I_{A0(1)}$ is based on phasor diagram (Fig. 1):

$$I_{A0(1)} = \frac{2RU_{a(1)} + \sqrt{4U_{A0(1)}^2\left(R^2+\omega^2L^2\right) - 4\omega^2L^2U_{a(1)}^2}}{2\left(R^2+\omega^2L^2\right)} \tag{31}$$

5.1. The Comparison of the analytical calculations and the simulations

In this chapter, the theoretical calculations are compared with the simulations. The Figures 10 and 11 show comparison of spectrums of the phase voltage of the active rectifier u_{A0} and comparison of the corresponding spectrums of current i_{A0}. It is obvious that, in accordance with the theory of the frequency modulation (16), the harmonics appear around the switching frequency and its multiples (f_{sw} = 800 Hz).

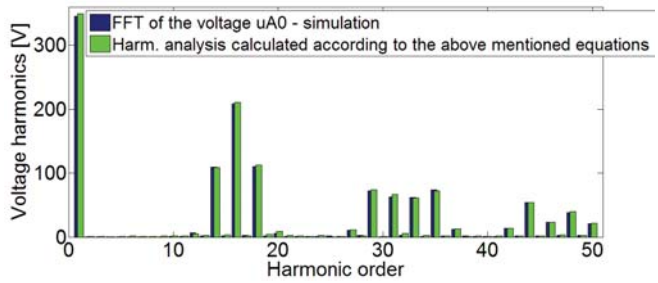

Fig. 10. Comparison of the spectrums of voltage u_{A0}

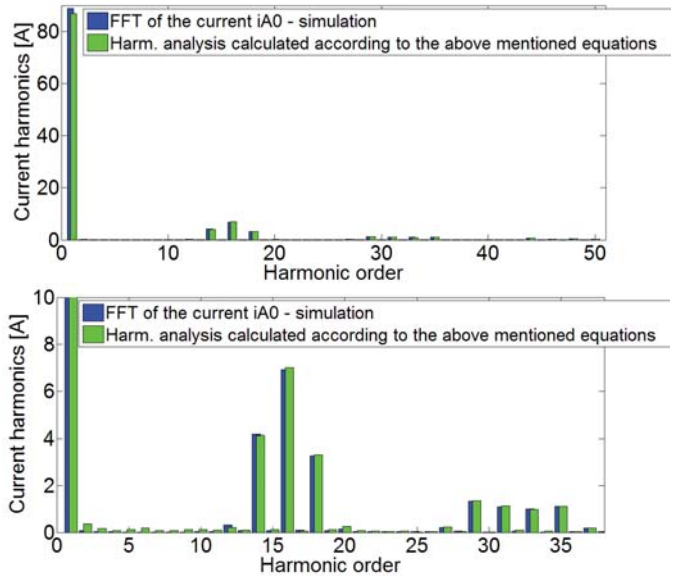

Fig. 11. Comparison of the spectrums of current i_{A0}

Individual harmonics of the currents i_{A0}, i_{B0} and i_{C0} are further summed according to the (32) in accordance with the phase shift of each harmonic components:

$$I_{a(h)} = \frac{1}{3}\left(2I_{A0(h)} - I_{B0(h)} - I_{C0(h)}\right) \tag{32}$$

The Figure 12 show spectrums of current drawn from the grid by the voltage--source active rectifier. It can be seen, that 16th harmonic equals zero in case of three--phase connection of active rectifier, because individual corresponding switching frequency harmonics of the currents i_{A0}, i_{B0} and i_{C0} are in the phase.

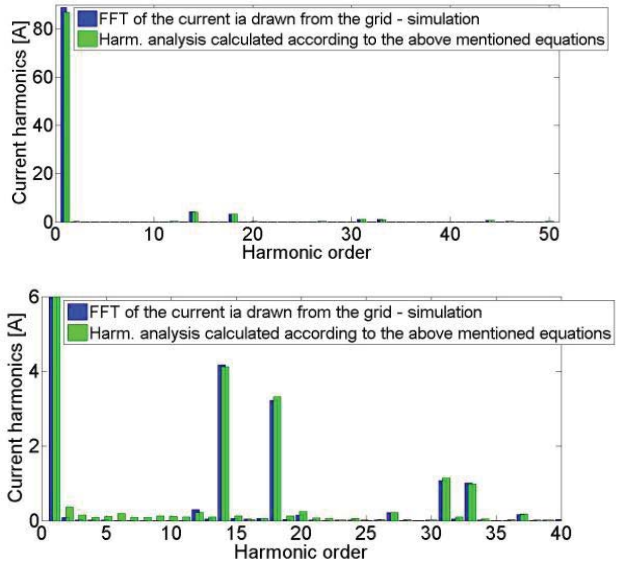

Fig. 12. Comparison of the spectrums of current drawn from the grid i_a

6. THE COMPARISON OF BOTH ANALYTICAL CALCULATIONS OF HARMONIC ANALYSIS

The next graphs (Fig.13) show the comparison of both analytical calculation of harmonic analysis with simulations. The switching frequency is 500 Hz.

The Figure 13 shows that the error rate of the both calculations performed according to the above stated formulas is very small and it is further proven that the harmonics appear around the switching frequency and its multiples (16). When the three-phase voltage-source active rectifier is connected, the harmonics that have the same frequency as the switching frequency or as the multiples of the switching frequency do not appear in the spectrum of the current drawn from the grid, because these harmonic components are in the phase.

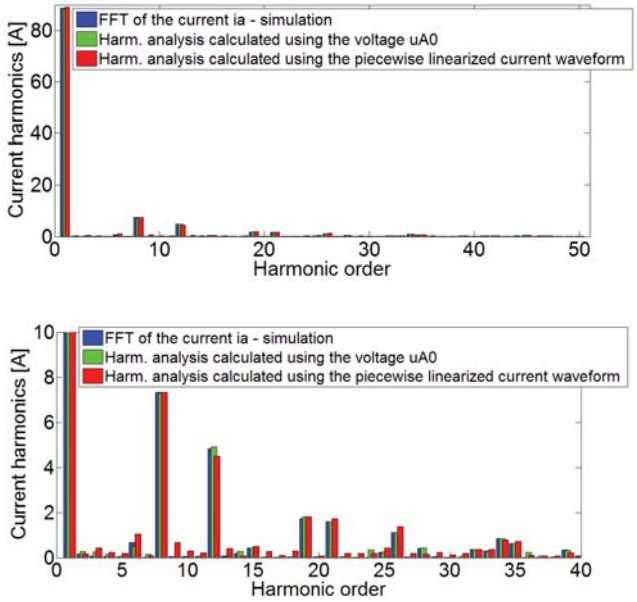

Fig. 13. Comparison both analytical calculations of harmonic analysis with simulations

7. CONCLUSION

This paper presents application of the theory of frequency modulation, which is used to determine the harmonics in the spectrum of the current drawn from the grid by voltage-source active rectifier. In accordance with Bessel functions it was confirmed, that the harmonics appear around the switching frequency of the pulse width modulation and its integer multiples.

The next part shows calculations of the amplitude of current harmonics using piecewise linearized current waveform. The graphs show that even in case of the simplified piecewise linearized current waveform the error rate of harmonic analysis is very small (less than 1%). In all graphs that show the spectrum of current we can see the most noticeable harmonics close to the switching frequency and its multiples.

In the next part the size of current harmonics is derived from voltage signal formed by pulse width modulation. Using this voltage, the equations for the first to h^{th} current harmonics are analytically calculated. These calculations are faster than the previous method of calculations.

This paper proves that the voltage-source active rectifier does not generate dangerous values of current harmonics. The danger of the active rectifier only consists in the fact that the resonant frequency of the grid, which the active rectifier is located in, may be identical with the frequency of PWM (switching frequency) of this active rectifier.

ACKNOWLEDGMENT

This paper was supported by the project No. GAČR 102/09/1164 and by the project SGS-2012-071.

LITERATURE

1. Kus V.: Impact of power electronic converters on power distribution network. Book edited in BEN-technická literatura. Praha, Czech Republic, 2002. (in Czech)
2. Kus V., Peroutka Z., Drábek P.: Non-characteristic harmonics and interharmonics of power electronic converters, 18th International conference and exhibition on electricity distribution, 2005 CIRED, Turin, Itálie.
3. Santarius P., Krejci P., Spacil D., Vasenka P.: Power quality problems in regional distribution networks in the Czech Republic, Electrical Power Quality and Utilisation. EPQU 2007. 9th International Conference, pp. 1-6, 9-11, Oct. 2007.
4. Akagi H.: Active Harmonic Filters, Proceedings of the IEEE, vol. 93, no. 12, pp. 2128--2141, Dec. 2005.
5. Kiss P., Dan A.: The application of the double domain simulation by different harmonic filtering methods of 25 kV electric traction systems, Harmonics and Quality of Power. ICHQP 2008. 13th International Conference, pp. 1-6, Sept. 28 2008 – Oct. 1 2008.
6. Kus V., Josefova T.: Harmonic Currents Generated by the Voltage-Source Active Rectifier, Power Engineering, Energy and Electrical Drives. POWERENG'13. International Conference, May 2013.
7. Blahnik V.: Peroutka Z., Molnar J., Michalik J.: Control of primary voltage source active rectifiers for traction converter with medium-frequency transformer, Power Electronics and Motion Control Conference. EPE-PEMC 2008. 13th, pp. 1535-1541, 1-3 Sept. 2008.
8. Kiss P., Balázs G.G., Dán A., Schmidt I.: The application of the double domain simulation with PWM controlled locomotives, Harmonics and Quality of Power (ICHQP), 14th International Conference, pp. 1-6, 26-29 Sept. 2010.
9. Malinowski M., Jasinski M., Kazmierkowski M.P.: Simple direct power control of three--phase PWM rectifier using space-vector modulation (DPC-SVM), Industrial Electronics, IEEE Transactions, vol. 51, no. 2, pp. 447-454, April 2004.
10. Howell K.: Principles of Fourier analysis. Boca Raton: Chapman & Hall, 2001. 776 s. Studies in advanced mathematics.
11. Bachman G., Beckenstein E., Narici L.: Fourier and wavelet analysis. New York: Springer, 2000. ix, 505 s. Universitext.
12. Kus V., Josefova T.: The Use of Theory of Frequency Modulation for the Calculation of Current Harmonics of the Voltage-Source Active Rectifier, Applied Electronics (AE), International Conference, September 2013. (contribution in the review proceedings)
13. Josefova T., Kus V.: Analysis of Current Drawn by the Voltage-Source Active Rectifier from the Electricity Network, Energetics (IYCE), Proceedings of the 2011 3rd International Youth Conference, June 2013. (approved contribution)
14. Holmes D.G., Lipo T.A.: Pulse width modulation for power converters: principles and practice. John Wiley & Sons, 2003.

15. Jenni F., Wuest D.: Steuerverfahren für selbstgeführte Stromrichter. Zürich, Stuttgart: vdf Hochschulverlag und B.G. Teubner, 1995.

Manuscript submitted 20.06.2013 r.

PORÓWNANIE DWÓCH SPOSOBÓW OBLICZEŃ HARMONICZNYCH PRĄDU POBIERANEGO Z SIECI ELEKTROENERGETYCZNEJ PRZEZ PROSTOWNIK AKTYWNY, STANOWIĄCY ŹRÓDŁO NAPIĘCIA

Vaclav KUS, Tereza JOSEFOVA

STRESZCZENIE *Prostownik aktywny eliminuje charakterystyczne harmoniczne prądu, które są pobierane z sieci elektroenergetycznej przez prostowniki diodowe (tyrystorowe). Artykuł przedstawia analityczną analizę prądu pobieranego z sieci elektroenergetycznej przez prostownik aktywny, stanowiący źródło napięcia. Pierwsza część omawia zasady działania prostownika aktywnego jako źródła napięcia. Następna część opisuje analizy prądu przeprowadzone dwoma sposobami, a kolejny fragment przedstawia porównanie wyników tych analiz z wynikami badań symulacyjnych.*

Słowa kluczowe: *prostownik aktywny, analiza harmoniczna, modulacja częstotliwości, analiza Fouriera*

Prof. Ing. Vaclav KUS is employee of the Department of Electromechanics and Power Electronics, Faculty of Electrical Engineering, University of West Bohemia, Pilsen, Czech Republic. He is head of this department.

The research area prof. Kus is in the interaction of power semiconductors converters to the electricity grid, in impact on the fed devices, in the design of the features to eliminate harmonics and in design of protective equipment to reducing overvoltage on the load. He has courses “EMC in the Low Frequency Disturbance”, “Electric Drives and Power Electronics” and “Mechatronics and Industrial Electronics”.

Ing. Tereza JOSEFOVA graduated from the Faculty of Electrical Engineering in 2012. Now she is doctoral student in the Department of Electromechanics and Power Electronics, Faculty of Electrical Engineering, University of West Bohemia, Pilsen, Czech Republic. Her research area is effect of pulse width modulation of semiconductor converters to harmonics.